

c.2



Lawrence Berkeley Laboratory

UNIVERSITY OF CALIFORNIA

RECEIVED

LAWRENCE
BERKELEY LABORATORY

EARTH SCIENCES DIVISION

MAR 2 1987

LIBRARY AND
DOCUMENTS SECTION

To be presented at the NWWA/NGWMA Conference on
Solving Ground Water Problems with Models,
Denver, CO, February 10-12, 1987

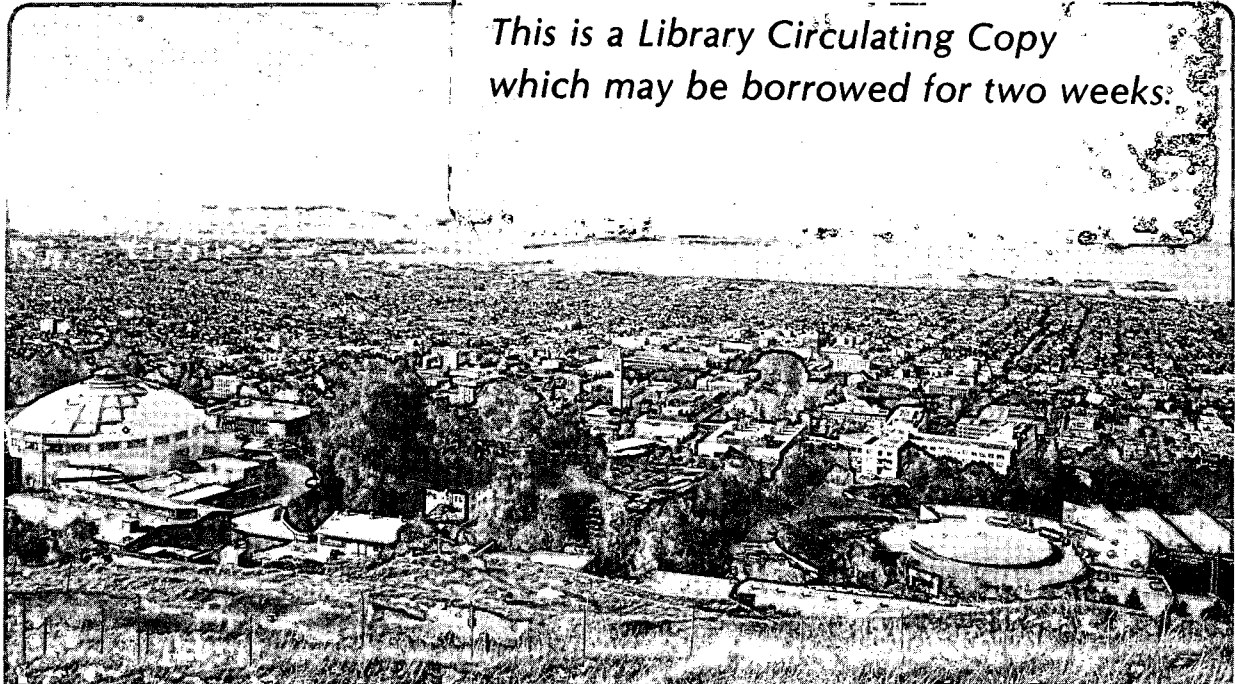
A NEW SEISMIC-HYDRAULIC APPROACH TO
MODELING FLOW IN FRACTURED ROCKS

P.A. Witherspoon, J.C.S. Long,
E.L. Majer, and L.R. Myer

January 1987

~~TWO-WEEK-LOAN-COPY~~

*This is a Library Circulating Copy
which may be borrowed for two weeks.*



LBL-22794

c.2

DISCLAIMER

This document was prepared as an account of work sponsored by the United States Government. While this document is believed to contain correct information, neither the United States Government nor any agency thereof, nor the Regents of the University of California, nor any of their employees, makes any warranty, express or implied, or assumes any legal responsibility for the accuracy, completeness, or usefulness of any information, apparatus, product, or process disclosed, or represents that its use would not infringe privately owned rights. Reference herein to any specific commercial product, process, or service by its trade name, trademark, manufacturer, or otherwise, does not necessarily constitute or imply its endorsement, recommendation, or favoring by the United States Government or any agency thereof, or the Regents of the University of California. The views and opinions of authors expressed herein do not necessarily state or reflect those of the United States Government or any agency thereof or the Regents of the University of California.

A NEW SEISMIC-HYDRAULIC APPROACH TO MODELING FLOW IN FRACTURED ROCKS

P. A. Witherspoon*, J. C. S. Long**, E. L. Majer** and L. R. Myer**

*Department of Materials Science and Mineral
Engineering, University of California, Berkeley,
California, and Earth Sciences Division, Lawrence
Berkeley Laboratory, Berkeley, California 94720

**Earth Sciences Division, Lawrence Berkeley
Laboratory, Berkeley, California 94720

Abstract

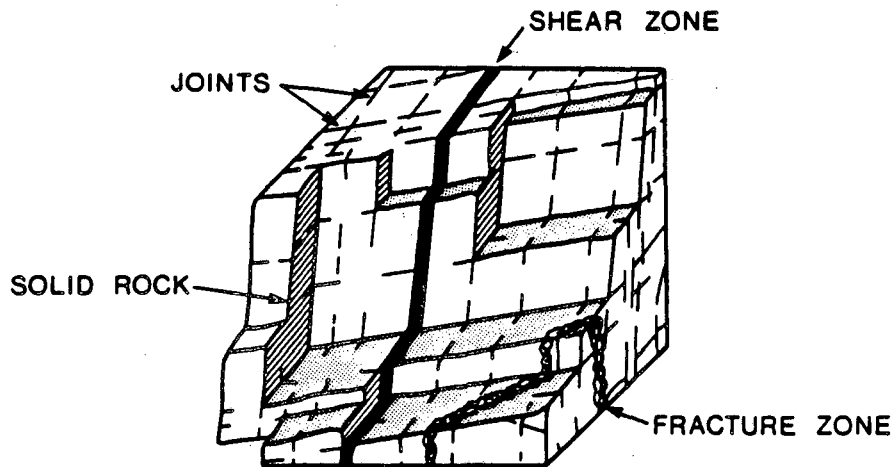
Modeling flow of ground water in fractured rocks is a major problem. This paper summarizes a program of investigations currently underway in this laboratory to characterize the geometry of fractured rocks and develop methods of handling flow in such systems. Numerical models have been developed to investigate flow behavior in two- and three-dimensional fracture networks. Two-dimensional studies of fracture interconnection indicate that systems with shorter fracture lengths have smaller permeabilities and behave less like porous media than those with longer lengths. Studies of transport indicate that the effects of increasing the coefficient of variation of aperture are opposite to those of increasing the correlation between length and aperture. Studies of scale and boundary effects indicate that the size of the representative elementary volume for homogeneously fractured systems may only be a function of fracture frequency. These are some examples of the insights to be gained from modeling studies of fractured rocks.

A key problem is gathering the necessary data on fracture geometry. Investigations have been started to determine how vertical seismic profiling (VSP) might be improved and applied to this problem. According to theory, a fracture can have a significant effect on shear wave propagation in rock systems. Laboratory measurements show a significant attenuation of shear waves as fracture stiffness decreases and frequency increases. A VSP experiment in The Geysers

geothermal field where fracture orientation is known, produced shear wave splitting and velocity anisotropy in agreement with theory. The results suggest the potential application of 3-component, multi-source VSP data in determining fracture orientation and average spacing. A downhole seismic wave generator would greatly improve VSP, and we are developing such a device. A model of wave propagation in fractured rocks is being used to understand how seismic signature can be linked to results from hydrologic models. We believe that the seismic-hydraulic approach can greatly enhance an understanding of fluid flow and transport in fractured rocks.

Introduction

Ground water specialists have long been aware of the problems of producing water from fractured rocks. The flow behavior of the rock mass is usually controlled, or at least affected, in some complex manner by the presence of discontinuities. These discontinuities can consist of fractures, joints and shear zones; and as shown in Figure 1, they usually occur in sets or families with similar geometries.



XBL 7811-13109

Figure 1. Fractured rock mass.

The basic problem for the ground water hydrologist is how to predict the way in which water will flow through such a system. For example, the production of fluid from a rock mass where the matrix has a very low permeability may not be practical unless the wellbore encounters a sufficient number of fractures. The fracture network can provide a multitude of flow paths that connect to many parts of the rock mass and thus become the channels for water movement. But when the movement is restricted to a complex network of fractures, can one still treat the system as though it were porous media? If so, what field measurements should be made to demonstrate this? These are questions that are not easily answered.

In addition to the field of ground water, there are many other examples in the earth sciences of activities that must also deal with fractured rocks. Table 1 presents a list that is by no means complete of some of these activities. In some cases, the desired activity is enhanced by the presence of the fractures. This is especially true when we want to withdraw fluid from a well for some purpose. On the other hand, one may seek a rock system with as few fractures as possible in order to minimize the fluid flow. The pollution of water supplies comes to mind when the disposal of liquid wastes is being considered in some situation involving fractured rocks. But in all of these field activities, the same question keeps coming up. How is the fracture system going to be characterized so that its flow behavior can be predicted?

In the past ten years or so, a concerted effort has been developing to investigate the factors that control the flow of fluids in fractured rocks. It has been shown that if enough details of the fracture system geometry can be obtained, it is possible to deduce a great deal about the flow properties of the system. One of the drawbacks to this approach, however, is that the field data necessary to characterize the fracture geometry are not commonly available. Some new developments in fracture detection in the field of seismology may be able to change this picture significantly. The purpose of this paper is to show some examples of the insights that can be developed with a flow model of a fracture network and then describe a new seismic approach to the problem of obtaining the necessary field data for such a model.

TABLE 1.	
Field Activities Where Problems Occur With Rock Discontinuities	
Open pit mining	Subsurface mining
Solution mining	Insitu coal gasification
Petroleum exploitation	Geothermal exploitation
Dam construction	Underground construction
Toxic waste isolation	Nuclear waste isolation
Underground energy storage	Earthquake control

Hydraulic Approach to Fractured Rocks

Introduction

In analyzing the problem of fluid flow through a network of fractures where the rock matrix is essentially impermeable, there are two major issues: (1) determining the permeability of the fracture system, and (2) establishing whether or

not such networks behave like porous media. In the past, methods developed by Snow (1965, 1969) have been applied where the orientations and apertures of the fractures intersected by a borehole were determined in the field. The fractures were assumed to be infinite in length, and an equivalent porous medium permeability was then computed as an accumulation of individual fracture permeabilities.

It is often observed in the field that fractured rock masses contain sets of discontinuous fractures with a geometry that may resemble that shown in Figure 1. The fractures are finite in size, that is, they do not extend indefinitely within the same plane. As a result, the degree of interconnection between the assemblage of discontinuous fracture planes is a critical feature that contributes to the hydraulic conductivity of the total system. The density, or the number of fractures per unit volume of rock, is another important feature. It has been customary to treat the fluid movement within each fracture in terms of flow between two planar surfaces whose aperture could be determined and an individual permeability computed. Finally, the orientation will determine those directions along which the fluids may flow within the total rock mass. Thus, the characterization of a fracture system is considered complete when each fracture can be described in terms of its: (1) size, (2) location, (3) effective aperture, and (4) orientation.

Recent work in this laboratory by Pyrak-Nolte et al (1987) has revealed that when a fracture is closed under stress, areas of contact between the fracture surfaces produce a very complex flow regime. The fluid motion is controlled by an intertwined network of channels whose geometry varies considerably from place to place within the fracture. Earlier work by Iwai (1976) revealed that when apertures were less than 10 microns, the flow behavior in a fracture was no longer in agreement with the traditional cubic law. Deviations from the cubic law have been reported by others (Engelder and Scholz, 1981; Gale, 1982) and are presumably caused by channel flow (Pyrak-Nolte et al., 1987). However, for larger fractures (10 to 100 microns or more), the cubic law is perfectly valid (Witherspoon et al., 1980) which suggests that channel flow may be an important factor only in fractures of low permeability. The problem of characterizing fracture flow may therefore have to take channel flow into account in some cases. Tsang and Tsang (1986) have proposed that channel flow can be characterized by an aperture distribution function and a spatial correlation factor.

Modeling Techniques

In order to investigate the details of fluid flow in fracture networks, one must have an appropriate model for the system in terms of its basic parameters. By varying these parameters in a systematic way, one can develop an understanding of the controlling features of the flow system. Numerical codes have been developed in this laboratory for this purpose to provide sample fracture systems for two- and three-dimensional investigations. The results presented below

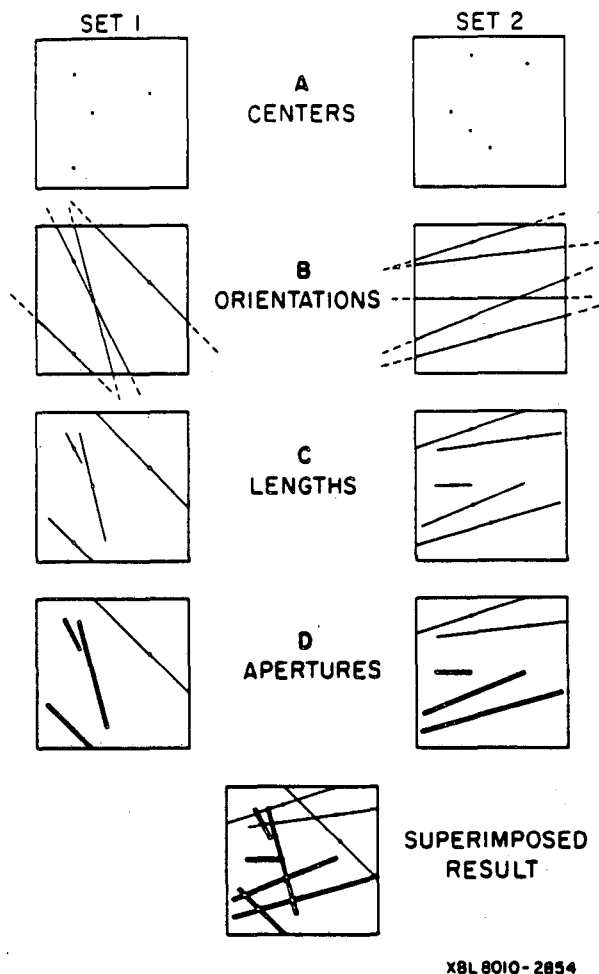


Figure 2. Generation of a two-dimensional fracture network (after Long, 1983).

are intended to illustrate how models can be used to investigate trends in the behavior of fracture systems.

The first effort was on two-dimensional problems, and a fracture mesh generator has been developed that produces random realizations of a population of fractures within a square area called a generation region (Long et al., 1982; Long, 1983). The code can handle several fracture sets, and each set is generated independently. The individual sets are superposed to create a network as illustrated in Figure 2. For each set, the density (number of fractures per unit area) must be supplied to determine the total number of fracture centers to be generated (Figure 2a). Then normally distributed orientations are randomly assigned to each center (Figure 2b). The fractures are randomly truncated such that the lengths are distributed according to a lognormal or negative exponential distribution (Figure 2c), and those particular fractures crossing the boundaries of the generation region are truncated at the boundary. Finally, lognormally

distributed apertures are randomly assigned to each fracture (Figure 2d), and the sets are superimposed. This process produces a fracture network similar to that proposed by Baecher et al. (1977). An example of a two-dimensional network is shown in Figure 3.

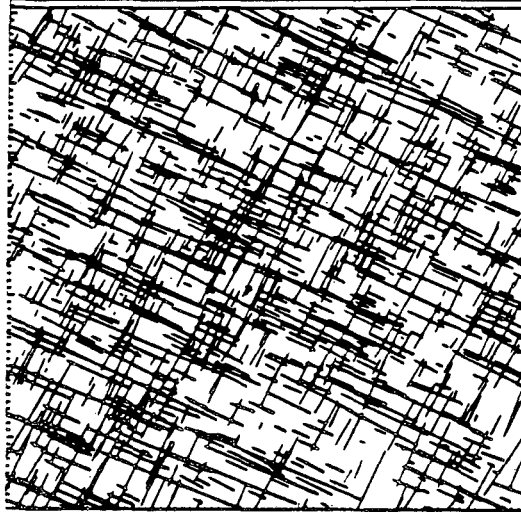


Figure 3. Example of two-dimensional network of fractures.

When all the sets have been generated, a flow region is selected for finite element analysis. The flow region is a square which is placed so as to be located entirely within the generation region with any arbitrary orientation. A hydraulic gradient is applied across the flow region by assigning appropriate values of head to the fractures where they intersect the boundary of the region (see Long et al., 1982, for details). Steady flux into the flow region in the direction of the gradient is calculated using a finite element program, LINEL, which was developed by Wilson (1970). Flux within each fracture is calculated using the cubic law and the rock matrix is assumed impermeable. Steady state flow through the network is calculated by solving a series of equations which guarantee that mass balance is maintained at each node of the network. The permeability in the direction of the gradient, K_g , can then be calculated from J , the magnitude of the total gradient, and Q_{in} , the total inflow to the system in the direction of the gradient:

$$K_g = Q_{in}/J \quad (1)$$

Permeability can be measured in any direction by rotating the boundaries of the flow region γ degrees and consequently rotating the direction of the gradient. For a homogeneous, anisotropic medium, $1/[K_g(\gamma)]^{1/2}$ versus γ is an ellipse when plotted on polar coordinates (Marcus and Evanson, 1961; Marcus, 1962; Bear, 1972). However, for inhomogeneous fractured media, $1/[K_g(\gamma)]^{1/2}$ may not plot as a smooth ellipse. In fact, as will be shown below, the shape of a plot using measured values of $K_g(\gamma)$ for a given test volume of rock may be quite erratic. This

plot can therefore be used as a test of whether or not the given rock can be approximated as a homogeneous porous medium. If $1/[K_g(\gamma)]^{1/2}$ does not plot at least approximately as an ellipse, then no single symmetric permeability tensor can be found to describe the medium. If the results cannot be described by a permeability tensor, flow through the medium cannot be analyzed with continuum techniques. Validation of this method of analysis can be found in the work of Long et al. (1982) and Long (1983).

Two-dimensional models developed by the procedures described above have a limitation in that fractures that are not connected to the network in the plane of analysis may in fact be connected in the third dimension. Thus, a two-dimensional analysis will tend to underestimate the permeability, and the network will appear to behave less like a continuum than it actually does in three dimensions. To overcome this limitation, the techniques described above have been extended to develop a model that can be used to calculate steady fluid flow in random three-dimensional fracture networks (Long et al., 1985; Gilmour et al., 1986).

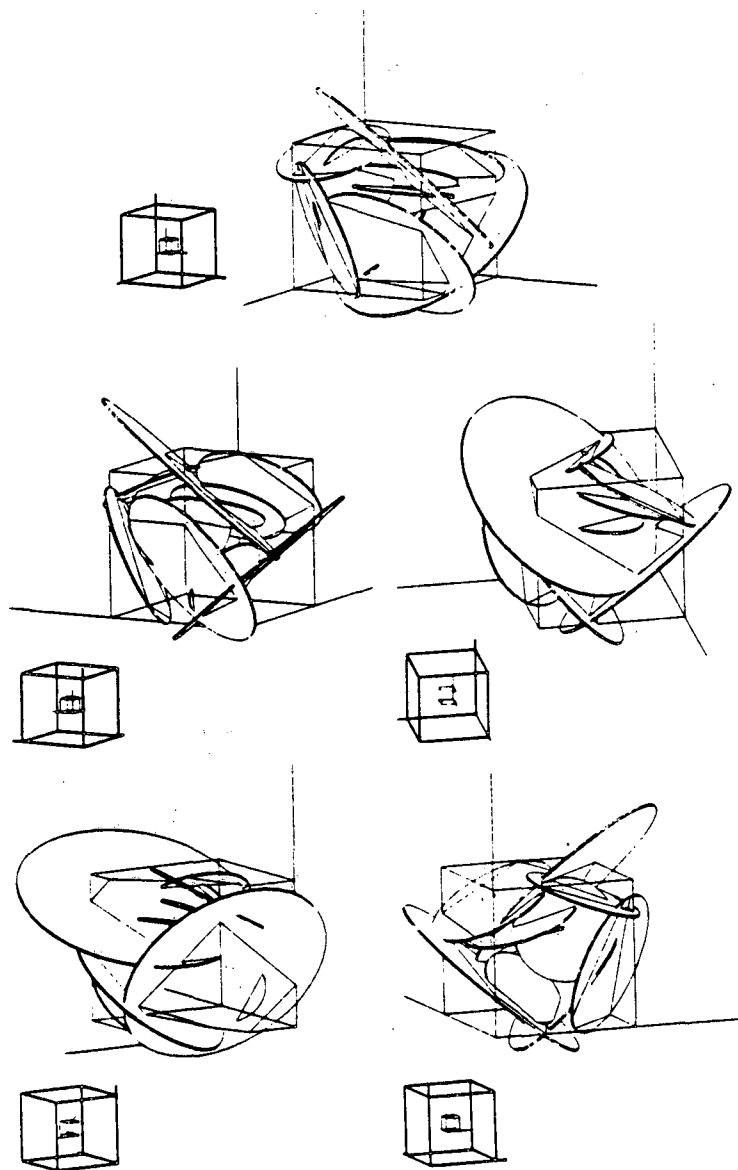
In developing a three-dimensional model of fracture networks, it is necessary that a conceptual model be adopted that is compatible with the geometry of fractured rocks in the field. From the analysis of trace data and examinations of fracture surfaces, several studies have shown that fractures are likely to be roughly elliptical or circular in shape (Robertson, 1970; Pollard, 1976; Baecher and Lanney, 1978). The assumption of a circular shape was adopted as a subset of the general elliptical case mainly because this shape simplifies the calculation of flow (Long et al., 1985; Gilmour et al., 1986). It was further assumed that the two opposite surfaces of the fractures are parallel and that the standard parallel plate model for flow is appropriate.

In this three-dimensional model, the disc-shaped discontinuities are assumed to be imbedded in an impermeable matrix, and the general treatment is similar to that developed for two-dimensional systems. The discs can be arbitrarily located within the rock volume and can have any desired distribution of aperture, radius, orientation, and density. Thus, where the disc model is appropriate, it is possible to calculate flow through fracture networks that are statistically similar to those that occur in nature. After a model has been generated, the intersections between discs are identified and the boundary conditions applied.

Steady flow through the network is calculated using a mixed analytical-numerical technique (Long et al., 1985; Gilmour et al., 1986). For each fracture, analytic equations are developed for flow into and out of each intersection with that fracture as a function of the average head at the intersection. The equations are based on image theory and the assumption that each intersection is a source (or sink) of uniform strength. A set of mass balance equations is necessary to equate flow into an intersection from one fracture and out to another fracture. These equations are solved using average values of head at each intersection, and

flux through the fractures can then be calculated by substituting the values of head back into the analytic equations. Details of the procedure including a description of three principal codes (FMG3D, DISCEL, and DIMES) that have been developed are given by Gilmour et al. (1986).

Figure 4 shows an example of a three-dimensional network that was generated using FMG3D for ten randomly located, random-sized fractures in a cubic flow region. In this example, the network was first generated within the large cube, and then a flow region was selected as shown by the smaller cube. The orientation of the fracture system within this flow region is illustrated from several different points of view.



ABL 969-11039

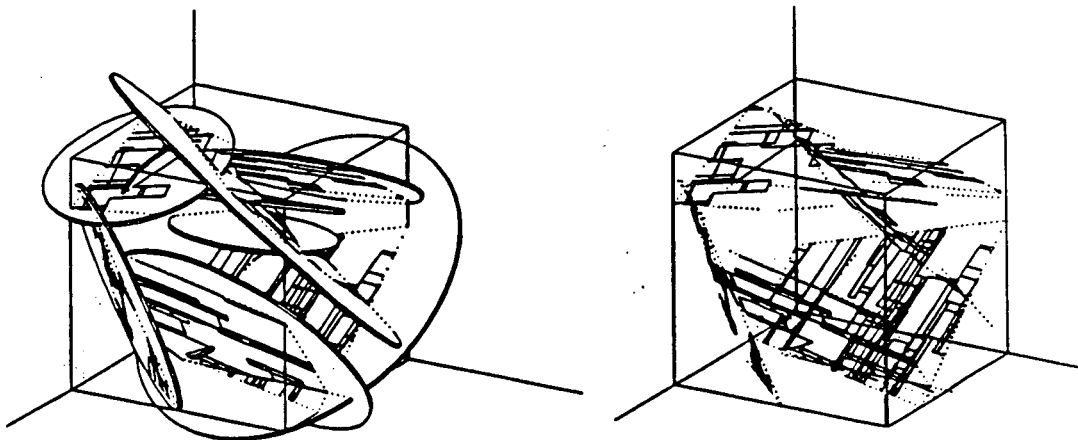
Figure 4. Example of three-dimensional network of fracture as seen from different viewpoints. (courtesy of D. Billaux).

Almost as soon as this three-dimensional model was completed, it became apparent that a further modification would enhance its utility in investigations of fractured rocks. As mentioned above, flux within any given fracture is calculated using the cubic law. In some cases, however, it may be necessary to treat the fluid movement in terms of channel flow. The three-dimensional model described above cannot, of course, account directly for channeling within the fracture planes. Billaux (personal communication, 1986) has therefore modified the three-dimensional model described above to include channel flow. The channels can be arbitrarily located within the fracture and can have any desired distribution of size, length, orientation and density. Figure 5a shows an example of a fracture model from the modified code where the orientation of a few randomly oriented fractures containing channels can be seen. In Figure 5b, the fractures have been removed to reveal the actual flow field that consists only of channels.

Research on the problems of transport in fractured rocks in both two- and three-dimensional systems is continuing using the various models described above. The following will illustrate the kind of results that have been obtained in this laboratory using models of two-dimensional systems where it has been assumed that the flux term in each fracture can be evaluated using the cubic law and some arbitrary value for the aperture.

Effect of Fracture Interconnection on Permeability

In order to study only the effect of fracture interconnection on permeability, Long and Witherspoon (1985) have examined two-dimensional networks of fractures where all the fractures in any given network had the same aperture and



XRL 8612-4927

Figure 5. Example of three-dimensional network: (a) showing fracture planes with channels; and (b) with fracture planes removed (courtesy D. Billaux).

length. Thus the networks were homogeneous, and any decrease in permeability from that which would be predicted by Snow's theory is due only to the lack of perfect connections between fractures. The aim of the study was to investigate the effect on permeability of those fracture parameters that cannot easily be measured in the borehole. In particular, the effect of varying the length and density of fractures was examined. Such a study is equivalent to an investigation of the degree of interconnection in a fracture network.

It is not necessary to examine all possible combinations of fracture length and density. For a given set of fractures it can be shown (Robertson, 1970; Baecher et al., 1977) that a probabilistic relationship for fracture frequency can be expressed by

$$\lambda_L = \lambda_A \overline{l \cos \theta} \quad (2)$$

where λ_L is the fracture frequency, i.e., the number of fractures in a given set per unit length of sample line; λ_A is areal density, which becomes volumetric density in three dimensions; \overline{l} is mean length, which becomes mean area in three dimensions; and θ is the angle between the sample line and the pole to each fracture of the given set. This equation implies that in two dimensions, the probability of a fracture intersecting a unit length of borehole is proportional to the areal density and the mean fracture length.

Unfortunately, λ and \overline{l} are difficult, if not impossible, to determine from an examination of borehole data. However, λ_L and θ can be measured so that if (2) is rearranged with knowns on one side and unknowns on the other, we have

$$\frac{\lambda_L}{\cos \theta} = \lambda_A \overline{l} = LD \quad (3)$$

Equation 3 means that for each set of fractures we may not be able to determine λ_A and \overline{l} directly, but we can estimate the product of these two terms because the left side of (3) can be determined from direct measurements in the borehole. This product will be called LD, or the length-density parameter.

In all of the following examples, the value of LD and the orientation distribution are the same. The values of λ_A and \overline{l} are varied such that the product $\lambda_A \overline{l}$ remains constant and equal to the chosen value of LD. Intuition tells us that if all else is held constant, an increase in fracture length will increase the permeability. Conversely, if all else is held constant, a decrease in fracture density will decrease the permeability. However, it is not immediately obvious how permeability will be affected if \overline{l} is increased by the same factor that λ_A is decreased.

The length-density study was carried out by Long and Witherspoon (1985) using systems where all fractures had the same aperture of 0.001 cm, and within any given system were uniform in length. Table 2 gives the parameters that were varied in order to investigate the effect of increasing length while keeping the product of length and density constant. The units used in all these studies are length in centimeters and hydraulic conductivity in centimeters per sec.

TABLE 2
Input Parameters Used in the Length-Density Studies

Name	Fracture Length l (Set 1 and Set 2) cm	Dimensions L x L cm	L/ l	Number of Fractures per Set per Unit Area λ_A , cm
LD2	2	12.5 x 12.5	6.25	0.1440
LD8	8	50.0 x 50.0	6.25	0.0360
LD10	10	62.5 x 62.5	6.25	0.0288
LD12	12	75.0 x 75.0	6.25	0.0240
LD14	14	87.5 x 87.5	6.25	0.0206
LD16	16	100.0 x 100.0	6.25	0.0180
LD20	20	125.0 x 125.0	6.25	0.0144
LD24	24	150.0 x 150.0	6.25	0.0120
LD64	64	140.0 x 140.0	2.34	0.0045

The length-density parameter LD was arbitrarily held at a fixed value of 0.288 cm^{-1} for all of these investigations. However, this approach could easily be scaled to represent a fractured rock having an LD of say 0.288 m^{-1} or about three fractures for every 10 m of borehole. What is important is the relative magnitude of the results not the absolute magnitude. Orthogonal fracture sets were used in all studies because if the sample size is sufficiently large, the theoretical shape of the permeability ellipse for orthogonal fractures of constant length and aperture is a circle. Thus, there should be no effects of anisotropy because the systems are isotropic. As shown in Table 2, the parameters of fracture length, flow region size, and fracture density were varied in a systematic manner. Input values of fracture density and length were calculated using

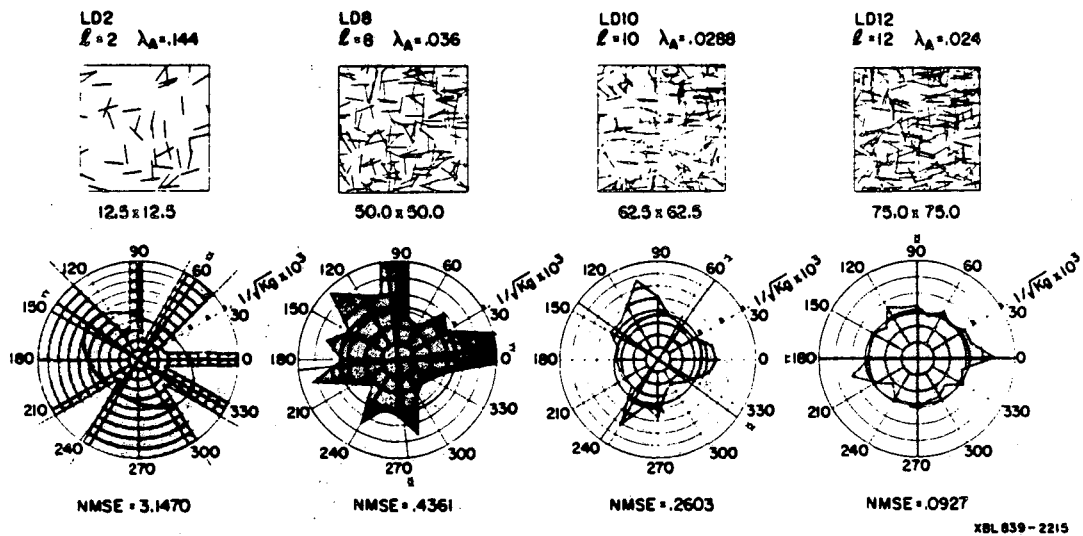
$$LD = \bar{l} \lambda_A = 0.288 \quad (4)$$

The effects on permeability of variations in length and density as one progresses from mesh LD2 to mesh LD12 are shown in Figure 6. In each figure the top half shows the networks used to calculate permeability. In each figure, only the 0° rotation is shown as an example, but for each model a total of six differently oriented flow regions were defined, and permeability was measured every 15° over a range of 360° .

The bottom half of Figure 6 shows the permeability ellipses for each network. The shaded areas represent the variation of the values of $1/(K_g)^{1/2}$ as calculated with the model, and it may be seen how erratic they become for small values of LD. Smooth ellipses have been superposed on the shaded areas to indicate the best fit to the data. The differences between the calculated results for a given fracture network and the permeability tensor that makes the best fit to the data are cast in terms of a normalized mean square error (NMSE). The pro-

cedure is similar to the regression technique used by Scheidegger (1954). The larger NMSE becomes, the less the fracture system behaves like a continuum, and if NMSE exceeds values of about 3, the system can no longer be treated like a porous medium. The values of NMSE are indicated beneath each LD result. The XX and YY values show the locations of the axes of the first and second principal permeabilities, respectively. The results for LD14 through LD24 are not shown but demonstrated a progressively closer and closer approach to the expected circle for isotropic behavior.

Each of the fracture meshes on Figure 6 are plotted using a different scale. The scale is varied such that each plot is the same size on the figure, but it will be remembered from Table 2 that the flow region size L is a constant multiple of 6.25 times the fracture length l . Thus, the fractures in all plots appear to be the same length when in fact they are not. Moving from $l = 2$ to $l = 12$ on Figure 6 actual fracture length l and the region size L are increasing, and for LD to remain constant, the areal density is decreasing. The net result is that the number of fractures in each mesh is increasing as l increases because it is easy to show that this number is given by $11.25 \times l$. If all the networks in Figure 6 were drawn to the same scale, it would be seen that there are actually more fractures per unit area in LD2 than in LD8, etc., and that the fractures in LD2 are shorter than those in LD8, etc.

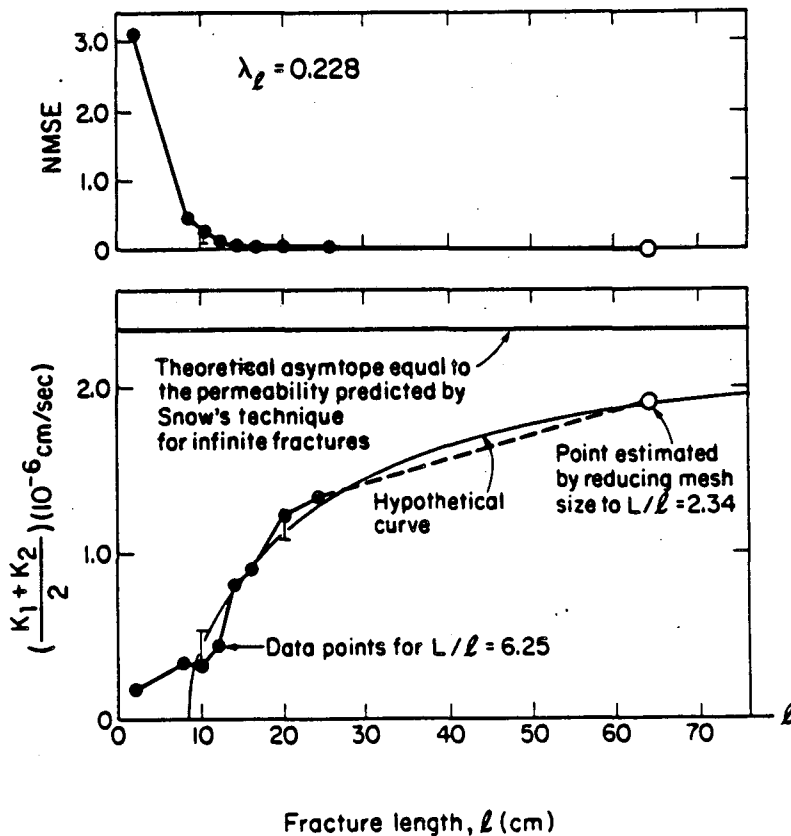


XBL 839-2215

Figure 6. Effects on permeability of variations in fracture length from 2 to 12 cm. Top half shows networks investigated and bottom half shows permeability results (after Long and Witherspoon, 1985).

Drawing all the meshes to the same size is useful because the "apparent density" has a strong influence on the hydrologic behavior of the fracture system. The longer the fractures, the higher the "apparent density" and consequently the higher the permeability. This is shown on Figure 7 where it appears that average K as a function of l increases rapidly as fracture length increases from 2 to 24 cm. Figure 7 also shows how NMSE varies as a function of length. The system has become connected for fracture lengths greater than about 8 cm. Once a sufficient degree of interconnection has occurred, further increases in fracture length cause the system to behave more like a porous medium as is evidenced by the low values of NMSE.

It also appears that the increase in K as a function of l is beginning to level off at higher values of l . This apparent decrease in the rate of change in permeability with increase in fracture length is very important. If for certain values of l , the permeability does not change very much, then it would appear that permeability can be predicted without knowing fracture length exactly. Therefore it



XBL8410-9991

Figure 7. Results of length-density studies showing effect of fracture length on permeability and NMSE (modified from Long and Witherspoon, 1985).

was important to find a way of projecting the results on Figure 7 for fracture lengths greater than $l = 24$ cm. Because of computer limitations at the time of the Long and Witherspoon (1985) investigation, the permeability of fracture systems with lengths longer than 24 cm could not be investigated using the constraint that $L/l = 6.25$ (see Table 2). To circumvent this problem, it was decided to reduce the L/l ratio from 6.25 to 2.34 because this made it possible to examine systems with fracture lengths of $l = 64$ cm. This resulted in a finite element mesh with approximately the same size as LD24 which was considered acceptable.

Figure 7 includes the result for the fracture length of 64 cm, and it may be seen that the permeabilities continue to increase over what was obtained for the investigations for LD2 through LD24 but at a decreasing rate. Using Snow's (1965, 1969) theory, one can easily calculate the permeability of a parallel system of fractures of infinite length with the spacing and aperture as used in this work. A value of $K = 2.35$ cm/s was obtained, and this is illustrated on Figure 7 by the horizontal solid line. Snow's (1965, 1969) technique should produce a theoretical maximum value for permeability, and it is evident on Figure 7 that the permeabilities obtained with the Long model are approaching the maximum value of Snow as l increases.

From the results of this length-density study (Long and Witherspoon, 1985), it would appear that when the fracture length is small, it must be measured in order to predict both permeability and behavior. Networks with shorter fracture lengths and higher density will have lower permeabilities than those with longer fracture lengths and lower density. Furthermore, systems with shorter fractures behave less like porous media than those with longer lengths. Thus, if a fracture system does not behave like a porous medium on one scale, increasing the scale of observation may not improve the behavior significantly. As fracture lengths increase, permeability approaches a maximum. This suggests that in systems with fractures longer than a certain minimum, it may not be necessary to require an exact measurement of length or areal density. Calculation of the maximum permeability using Snow's (1965, 1969) technique might be sufficient.

Effect of Fracture Aperture on Transport

One of the fundamental problems that is receiving more and more attention in hydrogeology is the transport of contaminants in ground water. Movement through fractured rocks presents additional difficulties because the continuum assumptions commonly applied to ground water systems are less likely to apply. To study this problem Long and Shimo (1986) carried out a numerical study using a fixed pattern of fractures in a two-dimensional network and investigated the effect of fracture aperture on transport. They used a single random arrangement of fractures and then examined the effect of variations in aperture distribution on the parameters used to characterize transport behavior: permeability, velocity, longitudinal dispersion and dispersivity length.

A single fracture pattern was generated in a two dimensional model using the numerical procedure described earlier. The flow region was 8 x 8 meters with a fracture density, λ_A , equal to 12 fractures per square meter. Fracture lengths were lognormally distributed with the mean and standard deviation equal to one meter. Fracture orientation was distributed uniformly from 0° to 360°, and flow was subjected to the same unit hydraulic gradient in all cases.

With the fracture pattern fixed, it was possible to investigate the effect of variations in aperture distributions. Fracture apertures were lognormally distributed with a mean, μ_b , and a standard deviation, σ_b . However, it was important that the fractures in each network have the same mean permeability; this was accomplished by requiring that the mean value of the cube of the aperture, $E(b^3)$, remain constant and equal to $(10^{-6}\text{m})^3$.

The fracture apertures were varied using two different procedures. In the first procedure, the coefficient of variation, $\nu_v = \sigma_b/\mu_b$, was allowed to vary from 0.0 to 1.5. In order to calculate the correct parameters for μ_b and σ_b , it was necessary to establish the relationship between these parameters and $E(b^3)$. Long and Shimo (1986) developed the expression:

$$E(b^3) = [\mu_b]^3 \left\{ \left(\frac{\sigma_b}{\mu_b} \right)^2 + 1 \right\}^3 \quad (5)$$

from which it is evident that in order to keep the mean value of b^3 constant while increasing ν_b , it is necessary to decrease μ_b .

In the second procedure, the coefficient of correlation between fracture length and aperture, C , was varied between 0.0 and 1.0. Three different degrees of positive correlation were tested such that apertures became larger as the length of the fractures increased. Correlations were achieved by randomly and independently choosing the values of fracture lengths and apertures. To achieve different degrees of correlation, these values were sorted by size into a number of corresponding groups. For example, apertures from 0 to 0.001 m were placed in one group, 0.001 to 0.002 m in the next group, etc. Fracture lengths were sorted in a similar manner, and an aperture was assigned at random to each fracture length from the corresponding group of lengths. The correlation coefficient was increased simply by defining a larger number of smaller groups.

The various combinations of ν_b and C that were used in generating fracture networks are summarized in Table 3. The letters B, C and D identify cases with an increase in the coefficient of variation, and the numbers 1, 2 and 3 identify cases with an increase in the correlation coefficient. The letter A refers to a special case of a network with a constant aperture, in other words, $\nu_b = 0$.

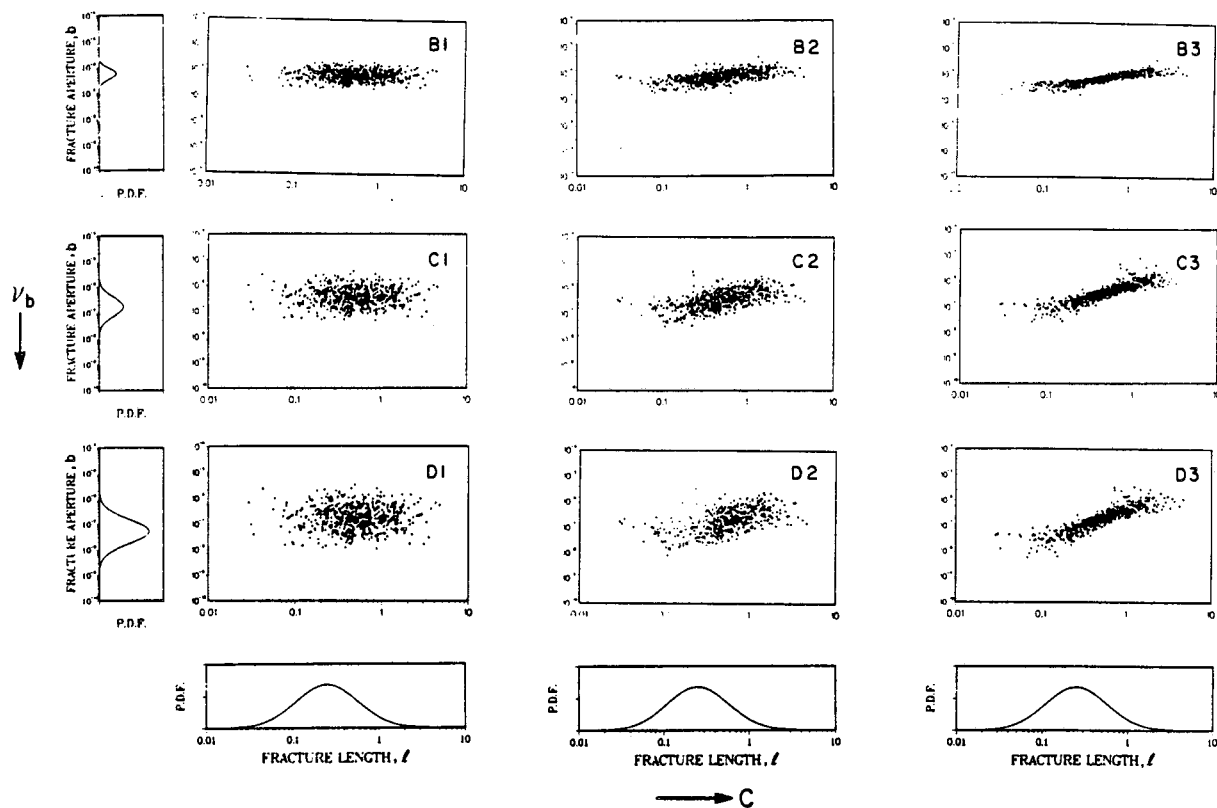
To investigate the transport characteristics of each of the ten systems listed in Table 3, Long and Shimo developed a numerical procedure for determining

		A	B	C	D
1	ν_b	0.0	0.5	1.0	1.5
	C		0.0	0.0	0.0
2	ν_b		0.5	1.0	1.5
	C		0.57	0.57	0.57
3	ν_b		0.5	1.0	1.5
	C		0.89	0.89	0.89

tracer transport when a pulse input moves through these systems. They assumed steady state flow conditions with complete mixing at fracture intersections. From the resulting tracer breakthrough curves, they determined the transport parameters: permeability, velocity, longitudinal dispersion, and dispersivity length. The details are given in their paper (Long and Shimo, 1986).

Long and Shimo developed a very interesting graphical representation of the various combinations of correlation versus aperture distribution, as shown in Figure 8. Case A is not shown because the aperture was constant and correlation has no meaning. An example of the fracture patterns that were generated for $\nu_b = 0.5$ is shown on Figure 9. The left side shows the effect of increasing C, the coefficient of correlation between length and aperture, from 0.0 to 0.89; the right side shows the same thing but with many of the non-conducting and isolated fractures removed.

Figure 10 presents the results of this analysis in terms of the transport parameters as a function of the coefficient of variation, ν_b , for the aperture distributions. The lines shown are for constant values of C. One notes immediately in Figure 10a the drastic reduction in hydraulic conductivity, or permeability, as the aperture distribution is allowed to spread (ν_b increases) even though the mean permeability of the fractures is constant. The permeability result for case A, the network with a constant aperture, is also included for comparison with B1, C1 and D1, for which $C = 0.0$. The apertures are not distributed in case A ($\nu_b = 0.0$), and it can be seen how the permeability reaches a maximum value when compared to the results of these three uncorrelated cases.

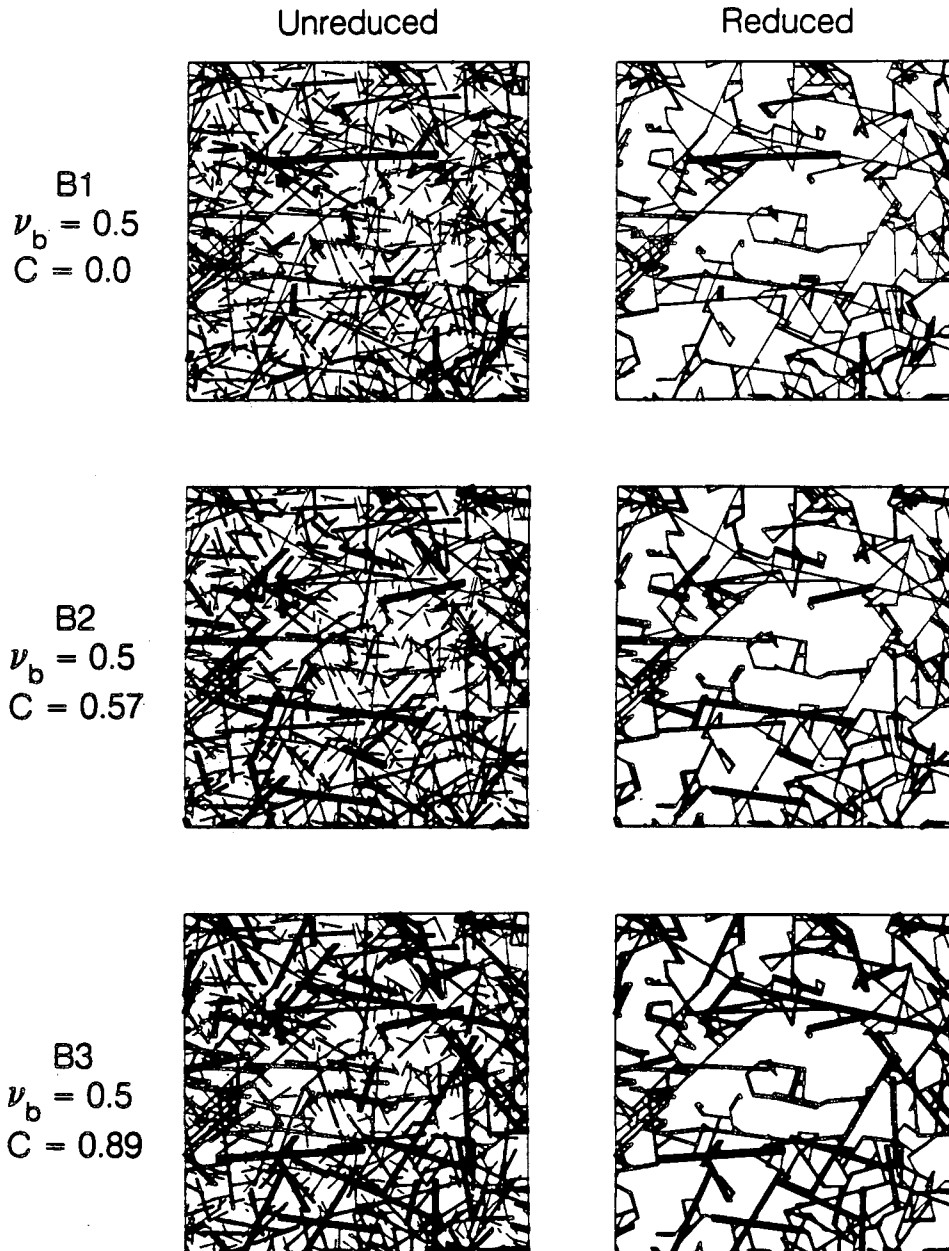


XBL 867-10899

Figure 8. Graphical representation of fracture distributions resulting from various combinations of length and aperture (after Long and Shimo, 1986).

The obvious effect in reducing network permeability as the aperture distribution increases is an important consideration. This is the result of the control on flux that is exerted by the smaller fractures in a discontinuous network. The more conductive fractures are fed by the smaller fractures, and thus, the larger conduits do not carry as much flux as they would if they transcended the entire flow region, that is, if they were infinite in size. The larger fractures are rendered less effective as conduits because of the way they are connected within the total system. One might think of this effect as simply the result of a decrease in fracture interconnection.

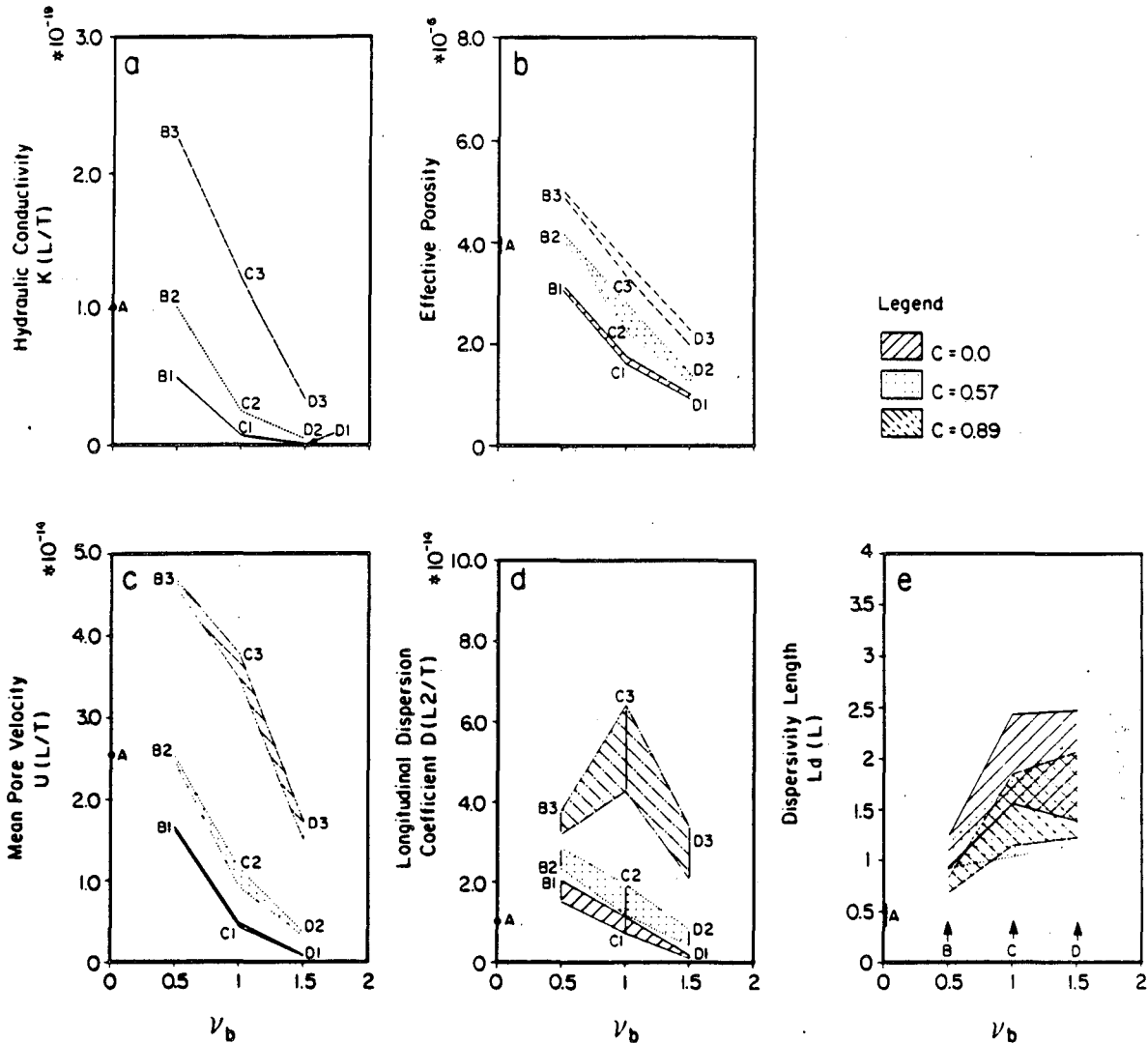
One also sees on Figure 10a how permeabilities are increased as the correlation between fracture length and aperture increases. The results become significant as the coefficient of variation increases. For example, when ν_b is 0.5 and the correlation coefficient is 0.89, the permeability is about four times greater than when the correlation coefficient is zero. However, when ν_b is 1.5, correlation increases the permeability by a factor of 50. It is evident that both of these coefficients are significant parameters in transport phenomena.



XBL 8512-12681

Figure 9. Example of fracture patterns (after Long and Shimo, 1986).

Figure 10b shows how the porosity decreases more or less proportionally with an increase in the coefficient of variation. It will be remembered from equation 5, that in order to keep $E(b^3)$ constant while increasing ν_b , it was necessary to reduce μ_b . Thus, because the mean aperture is decreasing, the porosity also decreases. An opposite effect occurs when the coefficient of correlation between



XBL 8512-12693

Figure 10. Transport parameters as a function of the coefficient of variation of aperture, ν_b , for constant values of the correlation between length and aperture: (a) hydraulic conductivity; (b) effective porosity; (c) pore velocity; (d) longitudinal dispersion coefficient; and (e) dispersivity length (after Long and Shimo, 1986).

length and aperture increases. In this case, porosity increases as C increases because the larger apertures are assigned to the longer fractures.

In analyzing the tracer breakthrough curves, Long and Shimo (1986) used three different methods of evaluating the mean velocity, U , the dispersion coefficient, D , and the dispersivity length, L_d . Figures 10c, d and e, respectively, show the results of this analysis as a function of the coefficient of variation, ν_b . Three bands are shown on each figure, one for each value of the correlation

coefficient, C . The width of each band shows the range of values obtained using each of the three methods. If all the different methods gave the same values for these parameters, it would mean that transport in the fracture network is the same as that of a theoretical porous medium. In other words, the conventional Fickian theory of dispersion would be applicable for analyzing transport. However, if the results obtained by these different methods show large discrepancies, the mechanism of mass transport through the fracture network must be different than that of porous media. The degree of the discrepancies would be a measure of the deviation from Fickian behavior.

It can be seen on Figure 10d that the dispersion coefficient tends to decrease as the coefficient of variation increases. This behavior is largely due to the fact that dispersion coefficient is proportional to velocity. It can be seen on Figure 10c that mean pore velocity decreases as the coefficient of variation increases. This is because the permeability is decreasing faster than the effective porosity.

One exception to a decreasing trend in dispersion coefficient with a variation in aperture is case C3. This is not easily explained. The peak at C3 may simply be a random fluctuation, or there may be some other maximizing effect in the statistics that creates a network structure that allows an early but narrow breakthrough of tracer followed by a long tail. One might envision this as occurring if there were a small number of highly conductive channels and also a number of poorly conductive channels.

The dependence of dispersion on velocity is eliminated by examining the dispersivity on Figure 9e. This figure shows that the dispersivity length generally increases as the coefficient of variation increases. Evidently, as the coefficient of variation increases from 0.5 to 1.0 to 1.5, the fracture systems become more and more heterogeneous. Thus, more and more different kinds of paths are available for tracer movement. Long and Shimo (1986) observed this in the tracer breakthrough curves.

As the correlation coefficient increases from 0.0 to 0.89, there is a tendency to get more mass through fewer high conductivity fractures. As a result, we see on Figure 10e that the dispersivity length becomes somewhat smaller as the correlation coefficient increases from 0.0 to 0.57, but not much smaller from 0.57 to 0.89. Apparently, the heterogeneities caused by aperture variation become somewhat better organized by an improving correlation between length and aperture, and this tends to offset some of the effects of dispersion.

The band widths on Figure 10 are indicative of how well the Fickian model applies to the breakthrough results for these fracture networks. Figure 10c shows that one can predict the mean pore velocity equally well for all methods of fitting the breakthrough curves. The same is not true for the dispersivity length, L_d . From an examination of the results on Figure 10e, it can be seen that the larger

the coefficient of variation and, to a lesser extent, the smaller the correlation coefficient, the less satisfactory is the Fickian model. Long and Shimo (1986) hypothesize that correlation between length and aperture has the effect of organizing the heterogeneities and creating less erratic behavior.

Long and Shimo (1986) have summarized the results of their investigation of the effects on transport of aperture dispersion and correlation between length and aperture as shown in Table 4. In all cases, the effect of an increase in the coefficient of variation for aperture is opposite to the effect of an increase in the correlation between length and aperture. On the basis of these results, they have suggested a methodology for treating homogeneously fractured rocks where the field data are limited to surface and borehole investigations.

Table 4.		
Effects on transport in fracture networks of aperture dispersion and correlation between length and aperture.		
	Increase in ν_b	Increase in C
Permeability	Decreases	Increases
Porosity	Decreases	Increases
Velocity	Decreases	Increases
Longitudinal Dispersion	Decreases	Increases
Dispersivity Length	Increases	Decreases (slightly)
Fickian Behavior	Decreases	Increases

The above investigations have focussed on the effects of fracture interconnection and fracture aperture. In more recent work, Long and Billaux (1986) describe a technique for processing field data which accounts for the observed spatial variability. This is done by generating a network subregion by subregion in which the properties of each subregion are predicted through geostatistics. Once the geometry of a particular network realization is specified, flow through the network is studied.

The problems of scale and boundary effects are currently being investigated by Long (1987). As larger and larger samples of the same network are examined, the permeability tends to approach an asymptotic value from above. The farther away the boundary conditions are applied relative to the sample of interest, the

more quickly the permeability asymptotes. All samples with the same fracture frequency appear to reach their asymptotic value of permeability at the same scale of measurement. Long (1987) interprets this as an indication that the size of the REV (Representative Elementary Volume) for homogeneously fractured systems may only be a function of fracture frequency.

Seismic Approach to Fractured Rocks

When sufficient details on the parameters of fractured rocks are available, it is evident from the above discussion that the use of models can provide valuable insights on the flow behavior. One of the obvious problems, however, is gathering the necessary data for such models. For that reason, we have begun a comprehensive series of investigations in this laboratory to determine how geophysical methods might be improved and applied to this problem. Our first efforts in this regard have been involved with a seismic approach to the problem of gathering data on the parameters of fractured rocks.

Seismic Properties of Natural Fractures

In recent theoretical (Schoenberg, 1980, 1983) and laboratory (Myer et al., 1985) investigations, a model has been developed that relates shear wave velocity and apparent attenuation to the "stiffness" of a fracture across which the displacement is not required to be continuous as a seismic wave passes. The discontinuity in displacement at the fracture is taken to be linearly related to the stress through the stiffness of the arrangement of asperities and voids. A fracture can thus have a significant effect on wave propagation. Schoenberg and others have shown that in a rock mass where fracture spacing is small compared to seismic wave length, the velocity ratio for propagation, perpendicular and parallel to the fracture set, is a function of spacing and stiffness of the discontinuities. Consequently, given the fracture stiffness, one should be able to use this model in determining average fracture spacing by measuring the velocity anisotropy.

Pyrak-Nolte et al. (1986) have recently reported the results of laboratory measurements on the attenuation of seismic waves passing across a single fracture. An example of results obtained with shear waves passing across a dry single fracture in a sample of dry granite is shown in Figure 11. The direction of propagation was perpendicular to the fracture and the normal stresses across the fracture ranged from 2.9 to 87.5 MPa. The frequency content of the propagating pulse ranged from about 0.1 to about 1.1 MHz.

The results of attenuation are presented in terms of a ratio of the shear wave spectral amplitude in the fractured sample relative to the spectral amplitude in the intact granite. Fracture stiffnesses were computed from measured fracture displacements, and over the stress range of 5 to 70 MPa, the specific stiffness increased by a factor of 10, from 2 to 22×10^{-6} MPa/m. One notes

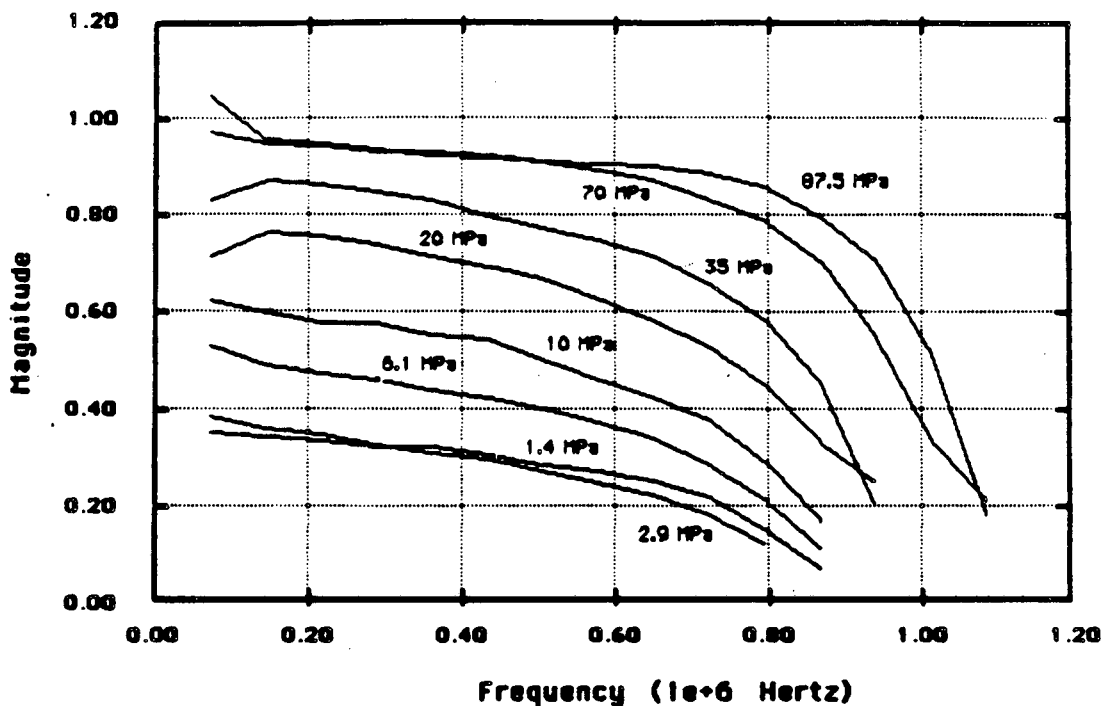
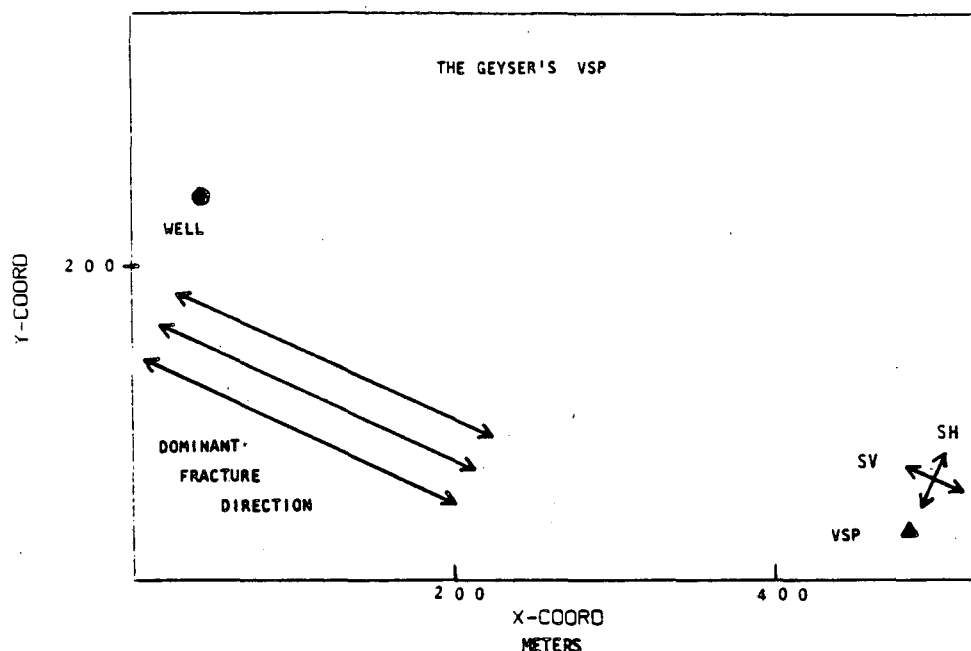


Figure 11. Attenuation of shear waves in propagating across a dry fracture in granite (after Pyrak-Nolte et al., 1987).

from the results on Figure 11 that there is a very significant attenuation of the shear waves as the fracture stiffness decreases, and as the frequency increases. These results are in good agreement with the theory of Schoenberg (1980, 1983).

Recent field investigations of seismic wave propagation have revealed another very important aspect of the seismic approach to fractured rocks. Majer et al. (1987) used compressional and shear wave sources with a 3-component geophone in a steam well at The Geysers geothermal field in northern California. The objective was to test the Vertical Seismic Profiling (VSP) technique in an area with well characterized fracture zones. Fracture content, dominant orientation and fracture spacing were the target parameters. Data were collected using P- and S-wave vibrators as sources. An innovation in this study was the use of orthogonal shear sources, which was accomplished by orienting the shear wave vibrator in two perpendicular directions for each geophone level in the steam well, to investigate anisotropy with the expectation that fracture properties would be reflected in shear wave velocity anisotropy. Peacock and Crampin (1985) have reported finding shear wave splitting in a transversely isotropic media using a shear wave vibrator oriented at various angles relative to the axis of anisotropy.

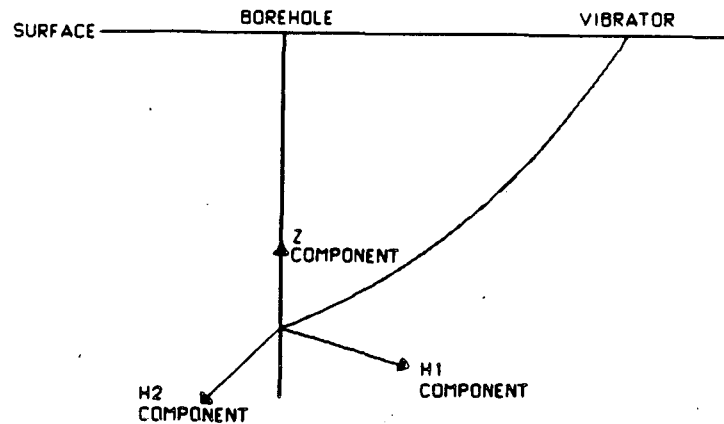
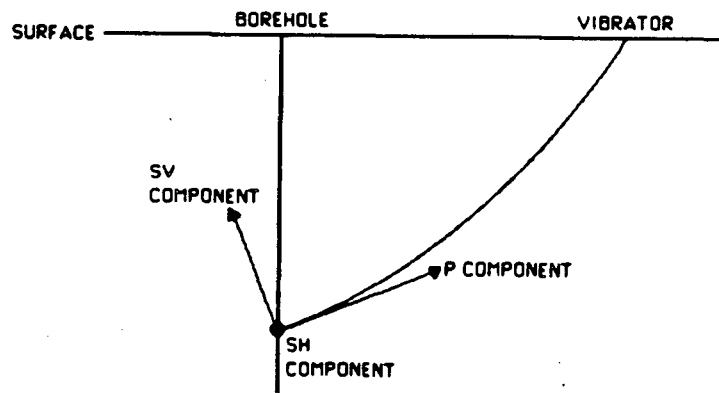


XBL 856-2834

Figure 12. Plan view of seismic survey layout relative to dominant fracture direction in The Geysers geothermal field. Shown are the locations of the steam well and VSP offset with directions of particle motion for shear wave sources (modified from Majer et al., 1987).

Figure 12 shows the layout of the field experiment and the orientation of the dominant fracture direction that has been revealed by drilling operations at The Geysers over the past several years. The depth to bedrock varies from zero to nearly 100 m at the site. A highly fractured greenstone caprock, 300 to 600 m thick, overlies a massive graywacke formation (McLaughlin, 1981). The location of the geothermal well in which the geophone was lowered at intervals of 30.5 m to a maximum depth of 1555 m is shown on the left side of Figure 12. The location of the shear wave vibrator with its two perpendicular orientations is shown on the right side at a distance of 518 m from the geothermal well. Locations of surface lines that were used to determine the utility of combined P- and S-wave profiles in identifying subsurface details are not shown. Details of the field operations and methods of data interpretation are given in Majer et al. (1987).

Due to the geometry of the source offset, the seismic wave energy arrived at an oblique angle to the borehole. The downhole 3-component geophone was oriented in the borehole to measure the seismic signals in the vertical, Z, and two orthogonal horizontal directions, H1 and H2. Ideally, one would like to replace the actual recording geometry with one that reflects the actual particle motion direction of the shear waves, as shown in Figure 13. The objective is to simulate the experiment one would have had if the borehole geophone were oriented with one component aligned on the incoming P-wave (called the P-component), a

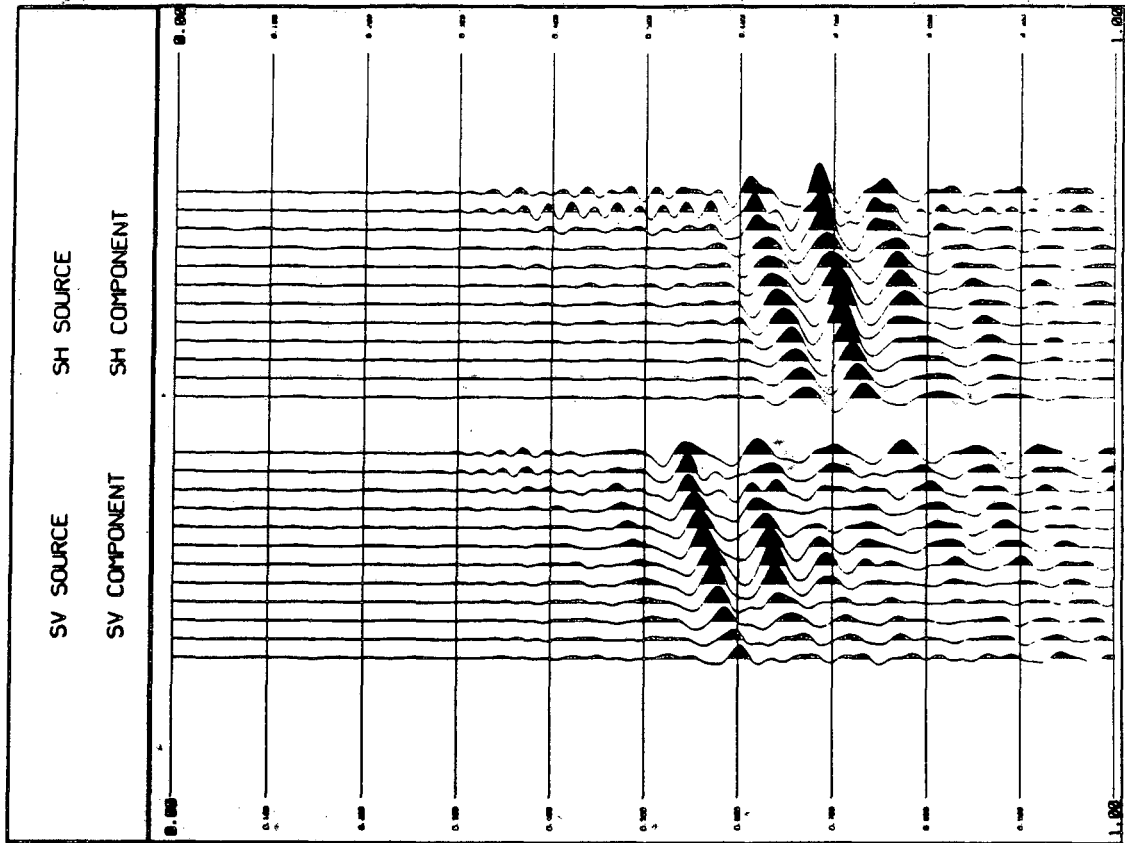
ACTUAL RECORDING GEOMETRYRECORDING GEOMETRY AFTER COORDINATE ROTATION

XBL 8511-4822

Figure 13. Graphical representation of geometry of seismic data as recorded and after coordinate rotation (after Majer et al. 1987).

second component in the vertical plane (SV-component), and the third component orthogonal to, and in the horizontal plane (SH-component). Majer et al. (1987) describe the polarization analysis that was carried out to accomplish this.

The transformed shear wave data provided important evidence of the effects of fractures on shear wave velocities. The SH source orientation produced a distinct SH arrival. On the other hand, the SV source orientation produced both SV and SH waves. The SH waves, however, were clearly different than that



XBL 8511-4830

Figure 14. Comparison of SH component from SH source with SV component from SV source. Total time span is one second and note difference of approximately 100 milliseconds in time of first arrivals (after Majer et al., 1987).

generated by the SH source, and this was confirmed by constructing particle motion hodograms (Majer et al., 1987). Figure 14 shows the relative arrival times of the SH component from the SH source versus the SV arrival from the SV source. The time span is one second, and it is evident that the travel time of the SH component is significantly more than that of the SV component. The velocity difference is 11 percent. Majer et al. concluded that the shear wave splitting and velocity anisotropy observed in this experiment provide dramatic field proof of the effects of fractures on the propagation of shear waves.

Majer et al. (1987) had planned to obtain similar data on three different azimuths at distances up to 900 m from the geothermal well. Presumably, if the direction of shear wave transmission were orthogonal to the dominant fracture direction instead of parallel, as in this field work (Figure 12), there would be no shear wave velocity anisotropy. One could then determine fracture orientation. Unfortunately, the downhole geophone was not designed for high temperature operation in a steam well, and the field work could not be completed as planned.

However, the results do suggest, as others have pointed out, the potential application of 3-component multi-source VSP data in determining fracture content and orientation. In addition, if the theory developed by Schoenberg (1980, 1983) relating SV and SH velocity differences to fracture stiffness is applicable, information on average fracture spacing may also be obtained.

Seismic Tomography of Fracture Networks

With the above results of seismic wave propagation through fractured rocks in mind, we have been pursuing a program of developing improved methods of vertical seismic profiling at the Lawrence Berkeley Laboratory. It has become quite clear to us, as well as many others, that the development of a downhole seismic wave generator would greatly enhance ones ability to traverse a rock mass with many different ray paths.

The basic idea is shown diagrammatically in Figure 15. By placing the downhole source at a desired location in one borehole and equipping a second borehole with a large number of 3-component oriented geophones, one can gather data for one set of multiple ray paths. By repeating the process with the source at a number of different depths, an enormous data base on the seismic response of the rock system can be generated. If other source wells are available at different azimuths from the borehole equipped with geophones, the seismic

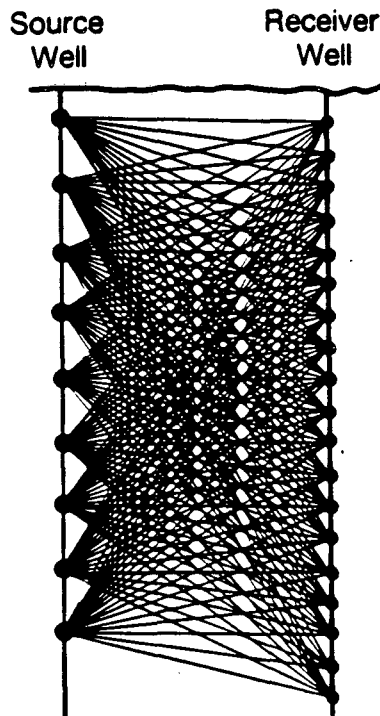


Figure 15. Seismic tomography with vibrator in source well and multiple geophones in receiver well.

response along other profiles should provide an even more complete picture.

There are no downhole seismic wave vibrators available commercially, although several groups are currently working on their development. We are working on the problem of developing an instrument that can generate both P- and S-waves and can be operated in a 7-inch cased hole. The most difficult part of this problem is the development of a device that can generate shear waves strong enough to traverse practical distances of one to two km and with high enough frequency content to provide adequate resolution. We are currently investigating the concept of using vibrating masses in the frequency range of 50 to 500 Hz to generate both SV and SH waves. SV waves can be generated by a mass that oscillates in an axial mode; and SH waves, by a mass that oscillates in the torsional mode.

In parallel with this instrumentation effort, we have also developed a numerical model of the process when P- and S-waves propagate through a fractured rock mass. The idea is to map the seismic tomography of an arbitrary rock system whose fracture density, orientation and size are known. It is necessary to know how the seismic signature depends on the fracture parameters of size, location, and orientation. One would also like to know how the seismic signature of a given system can be linked with the hydraulic response obtained using the methods described above. This would provide a seismic-hydraulic approach to fractured rocks.

The ultimate objective is to develop a methodology that can be applied to field problems on fractured rock systems. This will require boreholes to provide access to the underground for the seismic tomography. Fracture logging and oriented cores taken during the drilling operations will greatly aid the interpretation of fracture geometry. One must have some measure of the permeability of the fracture system, and this can be obtained from well testing and pressure buildup analysis. Because of its importance, a very large effort has evolved as many workers have endeavored to develop methods of interpreting flow data from fractured rock systems (Odeh, 1965; Kazemi, 1969; Stretsova, 1983; Lai et al., 1983; Karasaki et al., 1985). Gringarten (1984) has summarized the theory and practice of interpreting well tests in fractured reservoirs with double-porosity behavior. We believe the appropriate combination of these different methods of investigation can be developed into a seismic-hydraulic approach that will greatly enhance our ability to characterize fractured rocks and lead to a better understanding of fluid flow and transport in fractured rocks.

Summary and Conclusions

This paper is a summary of a comprehensive program of investigations currently underway at the University of California and the Lawrence Berkeley Laboratory to characterize the geometry of fractured rocks and to develop

methods of handling fluid flow and transport through such systems. Numerical models have been developed for two- and three-dimensional networks of fractures, and these models can incorporate the vagaries of channel flow whenever that becomes necessary.

Two-dimensional models have been used to investigate effects of the various geometric parameters of fracture systems in controlling flow and transport. An investigation of the effect of fracture interconnection on the permeability of homogeneous systems was carried out in a length-density analysis and reveals the importance of fracture length. It would appear that when length is small, it must be measured, in order to predict permeability. As fracture length increases, permeability approaches a maximum value, and it may not be necessary to have an exact measurement. Also, systems with shorter fractures behave less like porous media than those with longer lengths.

Another investigation describes the effects on transport of aperture dispersion and the correlation between length and aperture. The results indicate that the effect on the transport parameters (permeability, porosity, velocity, longitudinal dispersion and dispersivity length) of an increase in the coefficient of variation of aperture is opposite to the effect of an increase in the correlation between length and aperture. In a more recent study on scale and boundary effects, the results indicate that the size of the REV for homogeneously fractured systems may only be a function of fracture frequency. These are examples of some of the insights that can be developed using model studies in the hydraulic approach to fractured rocks.

One of the obvious problems with this approach is gathering the necessary data for the modeling investigations. We have therefore begun a series of investigations to determine how geophysical methods might be improved and applied to this problem of defining the geometry of fracture systems. According to theory, a fracture can have a significant effect on seismic wave propagation in rock systems. The velocity ratio for wave propagation, perpendicular and parallel to a fracture set, is a function of the spacing and the stiffness of the discontinuities. Consequently, given the fracture stiffness, one should be able to use this effect in determining average fracture spacing by measuring compressional and shear wave velocity anisotropy.

Our investigations have been carried out in the laboratory and in the field. The laboratory results show a very significant attenuation of shear waves as the fracture stiffness decreases and as the frequency increases, in good agreement with theory. Field studies were carried out in The Geysers geothermal field in northern California using compressional (P) and polarized shear (S) wave sources with a 3-component geophone in a steam well. The field data provide important evidence of the attenuation effects of fractures on shear waves. The fractured greenstone caprock over the geothermal reservoir was found to exhibit an 11 percent variation between SH (S horizontal) and SV (S vertical) waves generated by

using two orthogonal polarizations of the vibrator orientation for each geophone level in the well. Shear wave splitting and velocity anisotropy observed in this field experiment provide proof of the effects of fractures on the propagation of shear waves.

It has become quite clear that the development of a downhole seismic wave generator would greatly enhance one's ability to generate vertical seismic profile data adequate for tomographic inversion. We are working on the problem of developing a device that can generate both P- and S-waves, operate in a 7-inch cased hole, and transmit enough energy to traverse practical distances of one to two km. In parallel with this effort, we are also developing a model of the propagation process when P- and S- waves move through a fractured rock mass. The idea is to develop an understanding how the seismic signature depends on the fracture parameters that are used in the hydrologic models. Such an approach is being investigated to determine the extent to which this kind of seismic mapping of fracture systems can be combined with the hydraulic approach to fluid flow. In combination with conventional data from well testing, it is believed that the seismic-hydraulic approach can greatly enhance our understanding of fluid flow and transport in fractured rocks.

Acknowledgments

This work was supported by the U.S. Department of Energy under contract No. DE-AC03-76SF00098.

References

- Baecher, G. B., N. A. Lanney and H. H. Einstein. 1977. Statistical description of rock properties and sampling. Proc. 18th U.S. Rock Mech. Symposium, pp. 5C1-1-5C1-8.
- Baecher, G. B. and N. A. Lanney. 1978. Trace length biases in joint surveys. Proc. 19th U.S. Rock Mech. Symposium, pp. 56-65.
- Bear, J. 1972. "Dynamics of Fluids in Porous Media." Elsevier, New York. 764 pp.
- Billiaux, D. 1986. Personal communication.
- Engelder, T. and C. H. Scholz. 1981. Fluid flow along very smooth joints at effective pressures up to 200 megapascals. Geophys. Monograph 24. Edited by N. L. Carter et al., Amer. Geophys. Union, pp.147-152.

- Gale, J. E. 1982. The effects of fracture type (induced versus natural) on the stress-fracture closure-fracture permeability relationships. Issues in Rock Mechanics, Proc. 23rd Symposium on Rock Mechanics. University of California, Berkeley, Calif. pp. 290-298.
- Gilmour, H. M. P., D. Billaux and J. C. S. Long. 1986. "Models for Calculating Fluid Flow in Randomly Generated Three-Dimensional Networks of Disc-Shaped Fractures, Theory and Design of FMG3D, DISCEL, and DIMES." Lawrence Berkeley Laboratory, LBL-19515. Berkeley, Calif. 143 pp.
- Gringarten, A. C. 1984. Interpretation of tests in fissured and multilayered reservoirs with double-porosity behavior: Theory and practice. *J. Pet. Tech.*, Apr. 1984, pp. 549-564. *Trans. Amer. Inst. Min. Met. Eng.*, v. 277.
- Iwai, K., 1976. "Fundamental Studies of Fluid Flow Through a Single Fracture", Ph.D. Thesis. University of California. Berkeley, Calif., 208 pp.
- Karasaki, K., J. C. S. Long and P. A. Witherspoon. 1985. A new analytical model for fracture dominated reservoirs. Paper SPE 14171 presented at 60th Annual Technical Conference and Exhibition, Soc. Pet. Eng., Las Vegas, Sept. 22-25, 1985.
- Kazemi, H. 1969. Pressure transient analysis of naturally fractured reservoirs with uniform fracture distribution. *Soc. Pet. Eng. J.*, Dec. 1969, pp. 451-462. *Trans. Amer. Inst. Min. Met. Eng.*, v. 246.
- Lai, C. H., G. S. Bodvarsson, C. F. Tsang and P. A. Witherspoon. 1983. A new model for well test data analysis for naturally fractured reservoirs. Paper SPE 11688 presented at 1983 California Regional Mtg., Soc. Pet. Eng., Ventura, Mar. 23-25, 1983.
- Long, J. C. S. 1983. "Investigation of Equivalent Porous Medium Permeability in Networks of Discontinuous Fractures." Ph.D. Thesis. University of California. Berkeley, Calif. 277 pp.
- Long, J. C. S., J. S. Remer, C. R. Wilson and P. A. Witherspoon. 1982. Porous media equivalents for networks of discontinuous fractures. *Water Resour. Res.*, v. 18, no. 3, pp. 645-658.
- Long, J. C. S. and P. A. Witherspoon. 1985. The relationship of the degree of interconnection to permeability in fracture networks. *J. Geophys. Res.*, v. 90, no. B4, pp. 3087-3098.

- Long, J. C. S., P. Gilmour and P. A. Witherspoon. 1985. A model for steady fluid flow in random three-dimensional networks of disc-shaped fractures. *Water Resour. Res.*, v. 21, no. 8, pp. 1105-1115.
- Long, J. C. S. and D. M. Billaux, 1986. From field data to fracture network modeling - An example incorporating spatial structure. Submitted to *Water Resour. Res.*
- Long, J. C. S. and M. Shimo. 1986. The control of fracture aperture on transport properties of fracture networks. Submitted to *Water Resour. Res.*
- Long, J. C. S. 1987. Permeability of statistically homogeneous fracture networks. In preparation.
- Majer, E. L., T. V. McEvilly, F. Eastwood and L. R. Myer. 1987. Fracture detection using P- and S-wave VSP's at The Geysers geothermal field. *Geophysics*, in press.
- Marcus, H. 1962. The permeability of a sample of an anisotropic porous medium. *J. Geophys. Res.*, v. 67, pp. 5215-5225.
- Marcus, H. and D. E. Evanson. 1961. "Directional Permeability in Anisotropic Porous Media." Contribution 31. Water Resour. Center, University of California, Berkeley. 105 pp.
- McLaughlin, R. J. 1981. Tectonic setting of pre-Tertiary rock and its relation to geothermal resources in The Geysers-Clear Lake area. U.S. Geol. Survey Professional Paper 1141, pp. 3-23.
- Myer, L. R., D. Hopkins and N. G. W. Cook. 1985. Effects of contact area of an interface on acoustic wave transmission characteristics, in *Research and Engineering Applications*, Balkenia, A. A., ed., Proc. 26th U.S. Symposium on Rock Mechanics, South Dakota School of Mines, v. 1, pp. 565-572.
- Odeh, A. S. 1965. Unsteady-state behavior of naturally fractured reservoirs. *Soc. Pet. Eng. J.*, Mar. 1965, pp. 60-64. Trans., Amer. Inst. Min. Met. Eng., v. 234.
- Peacock, S. and S. Crampin. 1985. Shear-wave vibrator signals in transversely isotropic shale. *Geophysics*, v. 50, no. 8, pp. 1285-1293.
- Pollard, D. D. 1976. On the form and stability of open hydraulic fractures in the earth's crust. *Geophys. Res. Letters*, v. 3, no. 9, pp. 513-516.

- Pyrak, L. J., L. R. Myer and N. G. W. Cook. 1985. "Determination of Fracture Void Geometry and Contact Area at Different Effective Stress." Paper presented at Fall 1985 Mtg., Amer. Geophys. Union, San Francisco, Calif. Dec. 9-12.
- Pyrak-Nolte, L. J., N. G. W. Cook and L. R. Myer. 1986. "The Effect of Stress on the Hydraulic, Mechanical and Seismic Properties of a Natural Fracture." Paper presented at Spring 1986 Mtg., Amer. Geophys. Union, Baltimore, Md. Apr. 19-23.
- Pyrak-Nolte, L. J., N. G. W. Cook, L. R. Myer and P. A. Witherspoon. 1987. "Hydraulic and Mechanical Properties of Natural Fractures in Low Permeability Rock." Paper to be presented at 6th International Congress on Rock Mechanics, Montreal, Canada, Aug. 30 - Sept. 3.
- Robertson, A. 1970. The interpretation of geological factors for use in slope stability. "Proc. Symposium on the Theoretical Background to the Planning of Open Pit Mines with Special Reference to Slope Stability." South African Institute of Mining and Metallurgy. Johannesburg, South Africa. pp. 55-71.
- Scheidegger, A. E. 1954. Directional permeability of porous media to homogeneous fluids. *Geofis. Pura Appl.*, v. 28, pp. 75-90.
- Schoenberg, M. 1980. Elastic wave behavior across linear slip interfaces. *J. Acoust. Soc. Amer.*, v. 68, no. 5, pp. 1516-1521.
- Schoenberg, M. 1983. Reflection of elastic waves from periodically stratified media with interfacial slip. *Geophys. Prosp.*, v. 31, pp. 265-292.
- Snow, D. T. 1965. "A Parallel Plate Model of Fractured Permeable Media." Ph.D. Thesis. University of California. Berkeley, Calif. 331 pp.
- Snow, D. T. 1969. Anisotropic permeability of fractured media. *Water Resour. Res.*, v. 5, no. 6, pp. 1273-1289.
- Stretsova, T. D. 1983. Well pressure behavior of a naturally fractured reservoir. *Soc. Pet. Eng. J.*, Oct. 1983, pp. 769-780. *Trans. Amer. Inst. Min. Met. Eng.*, v. 275.
- Tsang, Y. W. and C. F. Tsang. 1987. Channel model of flow through fractured media. *Water Resour. Res.*, in press.
- Wilson, C. R. 1970. "An Investigation of Laminar Flow in Fractured Porous Rocks." Ph.D. Thesis. University of California, Berkeley, Calif. 178 pp.

Witherspoon, P. A., J. S. Y. Wang, K. Iwai and J. E. Gale. 1980. Validity of cubic law for fluid flow in a deformable fracture. *Water Resour. Res.*, v. 16, no. 6, pp. 1016-1024.

This report was done with support from the Department of Energy. Any conclusions or opinions expressed in this report represent solely those of the author(s) and not necessarily those of The Regents of the University of California, the Lawrence Berkeley Laboratory or the Department of Energy.

Reference to a company or product name does not imply approval or recommendation of the product by the University of California or the U.S. Department of Energy to the exclusion of others that may be suitable.

*LAWRENCE BERKELEY LABORATORY
TECHNICAL INFORMATION DEPARTMENT
UNIVERSITY OF CALIFORNIA
BERKELEY, CALIFORNIA 94720*